Competition of Acousto-Optical Polarization Rotation and Second Harmonic Generation in Periodically Poled Lithium Niobate

Kong Yan　Zhu Huaxin　Gao Shumei

(*Department of Optical Information Science and Technology*, *School of Science*, *Jiangnan University*, *Wuxi*, *Jiangsu* 214122, *China*)

Abstract Wave-coupling equations including acousto-optical (AO) polarization rotation and frequency doubling in periodically poled lithium niobate (PPLN) are proposed. The acoustic wave could either be induced from an external transducer or self-generated in PPLN driven with a cross-field radio frequency field. The proper reciprocal of PPLN is used to compensate the second harmonic generation (SHG) wave-vector mismatching, while phonon with suitable frequency may affect the pump polarization by scattering photons. Numerical simulation shows that there is a competition between the AO polarization rotation and SHG in PPLN under the phase-matching condition. The influences of the acoustic wave intensity on the polarization or intensity of three waves are studied.

Key words nonlinear optics; acousto-optical effect; second harmonic generation; quasi-phase matching

OCIS codes 190.4360; 230.1040; 190.2620

周期性极化铌酸锂中声光偏振旋转与倍频之间的竞争效应

孔　艳　朱华新　高淑梅

(江南大学理学院光信息科学与技术系，江苏 无锡 214122)

摘要 给出了在周期性极化铌酸锂晶体中同时包含声光调制和倍频产生的耦合波方程。声波既可以通过外部的换能器馈入，又可以通过在 y 方向加上交流电场而在铌酸锂晶体内部直接激发。周期性极化铌酸锂的周期倒格矢用于补偿倍频的波矢失配量，而合适频率的声子则通过光子散射来改变抽运光的偏振态。模拟结果显示，在相位匹配的条件下声光偏振耦合与倍频直接存在着竞争效应。三个光波的强度或者偏振态可以通过声光作用得到有效的调制。

关键词 非线性光学；声光效应；二次谐波产生；准相位匹配

中图分类号 O734^{+}.1　　**文献标识码** A　　**doi**: 10.3788/LOP50.111902

1　Introduction

Periodically poled lithiumniobate (PPLN) was extensively studied in the past decade for quasi-phase-matching (QPM) nonlinear interactions[1-4]. In PPLN, the nonlinear optical coefficients are modulated periodically owing to the periodic domain structure. Besides the nonlinear optical coefficients, the piezoelectric coefficients and electro-optical coefficients can also be modulated[5-8]. When two or more parameters are modulated together, some coupling effects would occur.

In a real crystal, various coupling effects exist among the motions of electrons, photons and phonons. The electron-phonon interaction plays an important role in electrons′ state in a crystal. The photon-phonon interaction in photonic microstructure also have been investigated with some new "acousto-optical (AO)" properties, e.g., macro-polariton excitation and tunable band gap[8-9]. It would be very interesting to see how the photon-phonon interacts in nonlinear crystals, i.e., artificial QPM microstructures.

收稿日期: 2013-07-03; **收到修改稿日期**: 2013-08-15; **网络出版日期**: 2013-10-14

基金项目: 国家自然科学基金(21206053)、中央高校基本科研业务费专项资金(JUSRP111A20)

作者简介: 孔　艳(1979—)，女，博士，讲师，主要从事非线性光学及光电子器件等方面的研究。

E-mail: ykong80@163.com

In this paper, we study the photon-phonon interaction in a PPLN crystal. We find that the acoustic wave could make the pump wave (PW) polarization rotate. Therefore, it could affect the wave vector matching between fundamental wave (FW) and its second harmonic (SH). The power flow curves among the PW, FW and SH are investigated through coupling wave equations with two different methods to generate acoustic wave. Under the QPM conditions for both acousto-optical polarization coupling and second harmonic generation (SHG), there is a competition between the polarization coupling and SHG.

2 Theory and simulation

When an acoustic wave travels in a PPLN crystal, it results in deformation so that the domain boundaries are displaced periodically. In addition, the refractive index also changes due to the traditional elasto-optic effect. Its optical properties will be affected by the periodic index modulation. As the PPLN is a one-dimensional microstructure, the collinear-phonons may scatter the photons toward the backward direction, i. e., Bragg scattering, or forward direction with orthogonal polarization[10]. As the backward scattering requires extremely high acoustic frequency, here we only consider the AO polarization rotation and its effects. The phonon's wave vector could compensate the wave vector mismatching between ordinary and extraordinary beams. This polarization rotation effect may be realized for either FW or SH depending on the phonon's frequency. Here we assume the following cascading process: $\omega_{1y}\rightarrow\omega_{1z}$, $\omega_{1z}+\omega_{1z}\rightarrow\omega_{2z}$. The y-polarized PW is coupled to z-polarized FW by the AO polarization rotation, and then is frequency-doubled to z-polarized SH. The pump wave propagates along the x-axis with y-polarization direction. Similar to Ref. [11], staring from Maxwell's equations and employing the plane-wave approximation, the coupling equations can be deduced with consideration of both AO and SHG interactions,

$$\begin{cases}\dfrac{\mathrm{d}E_{1y}}{\mathrm{d}x}=-\mathrm{i}\dfrac{\omega_1}{4n_{1y}c}n_{1y}^2n_{1z}^2p_{41}SE_{1z}\exp(\mathrm{i}\Delta\beta_1x)\\ \dfrac{\mathrm{d}E_{1z}}{\mathrm{d}x}=-\mathrm{i}\dfrac{\omega_1}{4n_{1z}c}n_{1y}^2n_{1z}^2p_{41}SE_{1y}\exp(-\mathrm{i}\Delta\beta_1x)-\mathrm{i}\dfrac{\omega_1d_{33}(x)}{n_{1z}c}E_{2z}E_{1z}^*\exp(\mathrm{i}\Delta\beta_2x)\\ \dfrac{\mathrm{d}E_{2z}}{\mathrm{d}x}=-\mathrm{i}\dfrac{\omega_2d_{33}(x)}{2n_{2z}c}E_{1z}^2\exp(-\mathrm{i}\Delta\beta_2x)\end{cases},\quad(1)$$

where $d_{33}(x)=d_{33}f(x)$, $\Delta\beta_1=\boldsymbol{k}_{1y}-\boldsymbol{k}_{1z}-\boldsymbol{H}$, $\Delta\beta_2=\boldsymbol{k}_{2z}-\boldsymbol{k}_{1z}$. $E_{j\xi}$, $\omega_{j\xi}$, $\boldsymbol{k}_{j\xi}$ and $n_{j\xi}$ (the subscripts $j=1,2$ refer to FW and SH, respectively, and $\xi=y,z$ represent the polarization) represent the electric fields, the angular frequencies, the wave vectors and the refractive indices, respectively. c is the speed of light in vacuum. d_{33} is the nonlinear coefficient, and $f(x)$ is the structure function that is $+1$ or -1 for the positive or negative domain of the PPLN. $\boldsymbol{H}$ corresponds to the acoustic wave vector whose amplitude is H. $S=HA$ is the amplitude of acoustic wave induced strain[12], where A is the maximal displacement of a mass point in PPLN when acoustic wave propagates in it. A longitudinal acoustic wave along x-direction is considered. P_{41} is the corresponding elasto-optic coefficient.

In a PPLN crystal, the structure function $f(x)$ can be written as a Fourier series, $f(x)=\sum_m g_m\exp(-\mathrm{i}\boldsymbol{G}_mx)$, where $\boldsymbol{G}_m$ are the reciprocal vectors and g_m are the amplitudes of reciprocal vectors. The acoustic frequency is firstly fine tuned to realize the AO polarization rotation at $\Delta\beta_1=0$. Without loss of generality, the reciprocal $\boldsymbol{G}_2$ is adopted to compensate the nonlinear phase mismatching as $\Delta\beta_2=\boldsymbol{k}_{2z}-\boldsymbol{k}_{1z}-\boldsymbol{G}_2=0$. In this case, the coupling equations [Eq. (1)] can be simplified as

$$\begin{cases}\dfrac{\mathrm{d}A_{1y}}{\mathrm{d}x}=-\mathrm{i}K_1A_{1z}\\ \dfrac{\mathrm{d}A_{1z}}{\mathrm{d}x}=-\mathrm{i}K_1^*A_{1y}-\mathrm{i}K_2A_{2z}A_{1z}^*\\ \dfrac{\mathrm{d}A_{2z}}{\mathrm{d}x}=-\dfrac{\mathrm{i}}{2}K_2A_{1z}^2\end{cases},\quad(2)$$

with $A_j=\sqrt{\dfrac{n_j}{\omega_j}}E_j$, $K_1=\dfrac{\omega_1(n_{1y}n_{1z})^{3/2}p_{41}S}{4c}$, $K_2=\dfrac{d_{33}g_2}{c}\sqrt{\dfrac{\omega_1^2\omega_2}{n_{1z}^2n_{2z}}}$.

In this phase matching case, the AO polarization rotation and SHG no longer proceed alone but coupled together, which leads to a continuous energy transfer among the PW, FW and SH. As seen from Eq. (2), the right-hand side of the second equation is composed of two terms: one represents the polarization coupling gain and the other is the loss to generate SH. The competition between these two processes is governed by the coupling coefficients K_1, K_2 and their ratio. The numerical solution to Eq. (2) is done to study this coupled AO-SHG effect. We set the wavelength of

PW at 1550 nm and working temperature T at 25 ℃. The period of PPLN $\Lambda = 18.99$ μm is set to satisfy the QPM condition. $d_{33} = 25.2$ pm/V, $p_{41} = -0.05$. Considering of the optical damage threshold for a near-stoichiometric $LiNbO_3$ crystal, the pumping FW intensity is set to be 10 MW/cm^2.

The simulation results of Eq.(2) are plotted in Fig. 1. In the case of $K_1/K_2 \geqslant 1$ [Figs. 1(a) and (b)], numerical simulations show that the AO polarization is much stronger than SHG. The energy exchange between the y-polarized pump wave and z-polarized FW goes faster, while the energy of z-polarized FW is converted into the SH wave. Moreover, the intensity of SH improves rapidly when intensity of z-polarized FW is relatively high. Comparing Figs. 1(a) and (b), the whole processes are similar, but the energy exchange between y-polarized pump wave and z-polarized FH goes slowly in Fig. 1(b). That is caused by the decrease of K_1. Figure1(c) shows the situation for $K_1/K_2 = 0.1$. It can be seen that the majority of the energy stored in the y-polarized PW is transferred to the z-polarized FW, and then transferred to the z-polarized SH. 51% power could be transferred to z-polarized FW with 1 cm PPLN. Then its power drops and is converted to y-polarized SH. If the crystal is 2 cm, there will be almost no y-polarized PW left while z-polarized SH gets the most energy and z-polarized FW still holds very little energy. When $K_1/K_2 = 0.05 \ll 1$, as shown in Fig. 1(d), the AO polarization rotation is very weak. The energy exchange among the three waves goes very slowly. When the crystal is 2 cm, y-polarized PW and z-polarized SH almost have the same power, while z-polarized FW holds the less power. If the length of the crystal continues to increase, we can predict that the pump wave and SH will share the power and there is almost no z-polarized FW left.

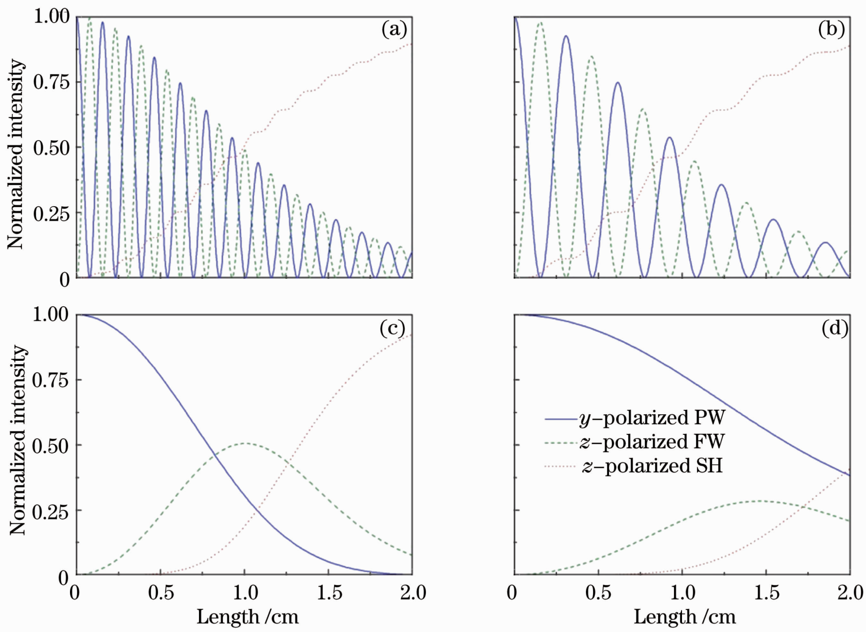

Fig. 1 Normalized light intensity versus PPLN sample length at different K_1/K_2 ratios. (a) 2; (b) 1; (c) 0.1; (d) 0.05

The three-wave output intensity and polarization depend not only on the ratio but also on the length of sample crystal. In Fig. 2, the three waves' intensities are plotted as functions of the ratio of the coupling coefficients K_1/K_2 with crystal length $x = 1$ cm. As we know, the frequency doubling coefficient K_2 is fixed when the crystal material and the period are determined, so that the ratio of the coupling coefficients K_1/K_2 can only be shifted by the polarization coupling coefficient K_1, which is related to the acoustic intensity. Due to the strong dependence of coupling behavior on the coupling coefficient ratio, a simple and convenient method for fast tuning the energy flow in PPLN can be employed by modulating the acoustic intensity.

In our simulation above, we assume the collinear propagated acoustic wave is coupled from an external transducer, which could be bonded directly to PPLN. However, in addition to nonlinear optical coefficient, the piezoelectric coefficient changes its sign periodically in PPLN, and it also could act as an acoustic superlattice to generate high-frequency bulk acoustic wave. One unique advantage of acoustic superlattice is cross-field excitation. The radio-frequency (RF) driving signals are applied at the sides of PPLN sample so that the refractive index and sound mismatching between the transducer and PPLN are solved. Normal metal electrodes could be used instead of transparent ones to get a simple and more reliable setup. This method with cross-field driving acoustic signal is more

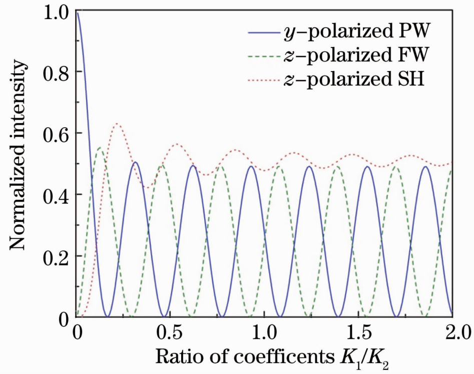

Fig.2 Normalized light intensity versus the ratio K_1/K_2 in a 1-cm-long PPLN sample

compact, simpler and more efficient than transducer.

A schematic diagram of the configuration is shown in Fig.3. A cross-field RF driving signal is applied at the y-side surface to excite longitudinal wave along the x-axis. When the phase-matching condition is satisfied for both AO polarization coupling and QPM frequency doubling simultaneously, the two processes are coupled together, i.e., $\Delta\beta_1 = \boldsymbol{k}_{1y} - \boldsymbol{k}_{1z} - \boldsymbol{H} = 0$, $\Delta\beta_2 = \boldsymbol{k}_{2z} - \boldsymbol{k}_{1z} = \boldsymbol{G}_2$. Obviously these conditions are difficult to be satisfied, giving tight constrains on working temperature, wavelength and superlattice geometrical parameter. For $LiNbO_3$ crystal, when the pump wavelength is set to be 1744.5 nm, the wave vector mismatching is $\Delta\beta_2 = 0.26093\ \mu m^{-1}$ at room temperature 25 ℃. In this case, a PPLN crystal with the period 24.08 μm and a symmetric duty cycle can be employed, and the corresponding acoustic frequency is $f = v/\Lambda = 0.273$ GHz.

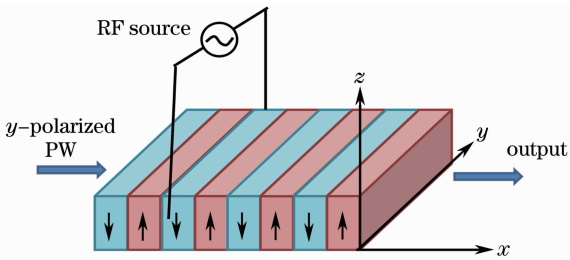

Fig.3 Schematic diagram of the AO polarization rotation and SHG in PPLN with cross-field RF driving

Figure 4 shows the calculated three-wave normalized intensity as a function of the acoustic wave′s amplitude. The PPLN length is 15 mm and the intensity of y-polarized pump wave is set to be 10 MW/cm^2, and the refractive indices of lithium niobate for different polarized waves are calculated from the Sellmeier data[13-14]. With the increase of acoustic amplitude, the AO polarization coupling process becomes rapid and z-polarized SH is increasing along with a reduction of y-polarized pump wave. The SH intensity doesn not reach its maximum when the y-polarized PW depletes completely. When the acoustic wave′s amplitude is about 1.25 nm, the SH gets its most energy. With the acoustic intensity going higher, the AO polarization rotation becomes stronger. Stronger acoustic wave destroys the satisfied QPM condition. The z-polarized FW has transferred its energy to y-polarized before z-polarized SH goes on grabbing energy from z-polarized FW. Thus SHG efficiency becomes lower.

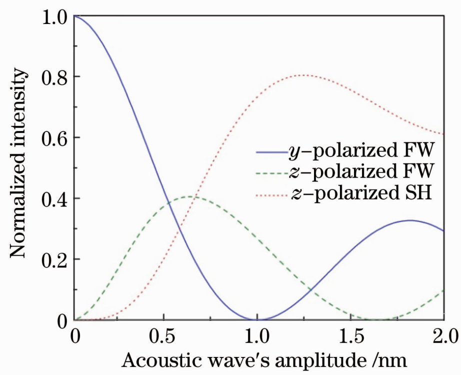

Fig.4 Normalized light intensities as functions of the acoustic wave′s amplitude in a 15-mm-long sample

From Fig.4, it can be concluded that the power and the polarization of three waves can be modulated by the acoustic intensity due to the competition between the AO polarization rotation and SHG. It should also be emphasized that the RF driving power or voltage is very low. For example, when the acoustic wave's amplitude A is 0.64 nm, z-polarized FW reaches its maximum, and the conversion efficiency of SH is 0.3682. The corresponding acoustic intensity is $I_a = 0.5\rho v^3 |HA|^2 = 18.35\ \mathrm{W/mm^2}$, where $\rho = 4640\ \mathrm{kg/m^3}$, $v = 5670$ m/s are used for calculation. Assuming a 0.5 mm×0.5 mm sample cross-section, the minimum required RF power is only 4.57 W. If the input impedance is 50 Ω, the driving voltage is only 39.88 V [root-mean-square (RMS) value].

3 Conclusion

In conclusion, we studied the photon-phonon interactions in PPLN. A united wave-coupling theory including AO polarization coupling and SHG was generalized. Numerical simulation shows that the different ratio K_1/K_2 could result in different power transfer among PW, FW and SH, which can be easily obtained by adjusting the acoustic wave intensity. Two effective ways to induce the acoustic waves were proposed, either by introducing an external transducer or self-generation in a PPLN acoustic superlattice. The external source selection is very flexible but the latter one is more efficient and convenient. This technique is particularly interesting for applications of both information transmission and frequency conversion.

References

1 V Berger. Nonlinear photonic crystal [J]. Phys Rev Lett, 1998, 81(19): 4136-4139.

2 L E Myers, R C Eckardt, M M Fejier, *et al.*. Multigrating quasi-phase-matched optical parametric oscillator in periodically poled $LiNbO_3$ [J]. Opt Lett, 1996, 21(8): 591-593.

3 Chen Dong, Li Wenqing, Zhang Yujn. Tuning characteristic of PPLN based difference-frequency-generation laser system [J]. Acta Optica Sinica, 2009, 29(3): 761-766.
陈　东，刘文清，张玉钧. PPLN晶体差频中红外激光系统调谐特性研究[J]. 光学学报，2009，29(3)：761-766.

4 Guo Shanlong, Han Yashuai, Wang Jie, *et al.*. Investigation of quasi-phase-matching frequency doubling of 1560 nm laser by use of PPLN and PPKTP crystals [J]. Acta Optica Sinica, 2012, 32(3): 0319001.
郭善龙，韩亚帅，王　杰，等. 1560 nm激光经PPLN和PPKTP晶体准位相匹配倍频研究[J]. 光学学报，2012，32(3)：0319001.

5 Y Q Lu, Zhi-liang Wang, Quan Wang, *et al.*. Electro-optic effect of periodically poled optical superlattice $LiNbO_3$ and its application [J]. Appl Phys Lett, 2000, 77(23): 3719-3721.

6 Xianfeng Chen, Jianhong Shi, Yuping Chen, *et al.*. Electro-optic Solc-type wavelength filter in periodically poled lithium niobate [J]. Opt Lett, 2003, 28(21): 2115-2117.

7 Kong Yan, Zhang Xiumei, Su Zhouping, *et al.*. Intensity and polarization modulation on cascaded frequency doubling and electro-optic coupling in periodically poled lithium niobate [J]. Laser & Optoelectronics Progress, 2012, 49(10): 101901.
孔　艳，张秀梅，苏宙平，等. 基于PPLN倍频-电光耦合级联的光调谐技术[J]. 激光与光电子学进展，2012，49(10)：101901.

8 Y Q Lu, Y Y Zhu, Y F Chen, *et al.*. Optical properties of an ionic-type phononic crystal [J]. Science, 1999, 284(5421): 1822-1824.

9 S Krishnamurthy, P V Santos. Optical modulation in photonic band gap structures by surface acoustic wave [J]. J Appl Phys, 2004, 96(4): 1803-1809.

10 H Gnewuch, N K Zayer, C N Pannell, *et al.*. Broadband monolithic acousto-optic tunable filter [J]. Opt Lett, 2000, 25(5): 305-307.

11 Zi-Yan Yu, Fei Xu, Fei Leng, *et al.*. Acousto-optic tunable second harmonic generation in periodically poled $LiNbO_3$ [J]. Opt Express, 2009, 17(14): 11965-11971.

12 A Yariv, P Yeh. Optical Waves in Crystals [M]. New York: Wiley, 1984. Chap. 9.

13 Dieter H Jundt. Temperature-dependent Sellmeier equation for the index of refraction, n_e' incongruent lithium niobate [J]. Opt Lett, 1997, 22(20): 1553-1555.

14 G J Ewards, M Lawrence. A temperature-dependent equation for congruently grown lithium niobate [J]. Opt Quantum Electron, 1984, 16(4): 373-375.